Egypt.J.Chem. **Vol. 63**, No. 2. pp.703-719 (2020)

Egyptian Journal of Chemistry
http://ejchem.journals.ekb.eg/

Electrochemical Behavior of Cu-10Al-10Zn Alloy in Seawater in the Absence and Presence of Benzotriazole Cationic Surfactants

M. A. Migahed[1], Ahmed. Nasser[2*], H. Elfeky[3], M.M. EL-Rabiei[3]
[1]*Egyptian Petroleum Research Institute, Nasr City 11727, Cairo, Egypt.*
[2]*Department of Basic Science, `High Institute for Engineering and Modern Technology, New-Elmarg, El-Qalyubia, Egypt.*
[3]*Chemistry Department, Faculty of Science, Fayoum University, Fayoum, Egypt.*

THE behavior of Cu-10Al-10Zn alloy in seawater was studied in absence and presence of different concentrations of different surfactants (1-hexyl-5-methyl-1H-benzo[d][1,2,3] triazole-1- ium bromide (HBT(6)), 1-dodecyl-5-methyl-1H-benzo[d][1,2,3]triazole-1- ium bromide, (DBT(12)), and 1-octadecyl-5-methyl-1H-benzo[d][1,2,3]triazole-1- ium bromide, (OBT(18)) as corrosion inhibitors. These inhibitors were synthesized and their structures, (HBT) as a representative compound, were confirmed using ^{1}HNMR and FTIR techniques. Conventional electrochemical techniques such as polarization methods and electrochemical impedance spectroscopy (EIS) were used. The inhibition efficiency increased by increasing the concentration of the prepared cationic surfactants in the medium. The curves of potentiodynamic polarization technique showed that, the performance of all prepared compounds act as mixed type. The standard free energy () values indicate that the three prepared cationic surfactants adsorbed via physicochemical adsorption and obeyed to Langmuir adsorption model. AFM technique observed the decrease of surface roughness due to the protective film formed on Cu-10Al-10Zn alloy surface.

Keywords: Cu-Al-Zn alloy, Seawater, Corrosion inhibition, Cationic surfactants, AFM, EIS

Introduction

Copper and copper alloys are industrially important materials due to unusual range of applications, especially in electrical wiring, cables and electrodes. They are also used in marine environments and saline water systems, e.g. heat exchangers and desalination plants, which can be considered now as an essential part of our daily life [1]. Corrosion and corrosion protection of copper and its alloys has engrossed a lot of attention and many studies have been conducted to date on this concern and are still on going. In highly aggressive environments which containing chloride and sulfate as corrosive ions, the possibility of passive film formation on copper alloys surface is low, and thus corrosion inhibitors are used to control corrosion rate in such environments [2]. Different types of inhibitors should be safe when used, besides being eco-friendly and economical [3,4]. The use of corrosion inhibitors founds one of the most economical ways to mitigate the corrosion rate, protect metal surface against corrosion and domain industrial facilities. The efficiency of any inhibitor is strongly associated to its chemical composition, concentration and the electrolyte solution [5]. Many classes of organic compounds were reported as effective corrosion inhibitors. Among them, some cationic surfactants especially including (quaternary ammonium salts).The adsorption ability of any surfactant can be enhanced by the presence of functional groups like double bond, benzene ring, nitrogen atoms in addition to hydrophobic chain of surfactant [6]. Azoles compounds is

*Corresponding author e-mail: ahmednasser1992@outlook.com; tel: 00201016526852
Received 3/6/2019; Accepted 2/7/2019
DOI: 10.21608/ejchem.2019.13443.1834

considered as one of the best compounds that have inhibiting action on the metals by bonding its surface with the free lone pairs of electrons of nitrogen atoms through P π—d π bond [7,8]. Benzotriazole (BTA) derivatives, for example, considered to be very useful inhibitors for several metals and alloys in different aqueous media [9-12]. To confirm this, the corrosion behavior of brass in the presence of two organic inhibitors that belong to the benzotriazole derivatives namely N-[1-(benzotriazol-1-yl) methyl] aniline (BTMA) and 1-hydroxy methyl benzotriazole (HBTA) has been investigated in neutral aqueous NaCl solution by using potentiodynamic polarization and electrochemical impedance spectroscopy (EIS) [13]. The results showed that all substituted benzotriazole derivatives indicate good inhibition efficiency in 3% NaCl medium and the order of inhibition efficiency: HBTA > BTMA > BTA. In the present paper, we are developing n-alkyl-quaternary ammonium salt based on benzotriazole as corrosion inhibitors, which improves the solubility of benzotriazole in seawater. Then the inhibition performance of the prepared compounds for the Cu-10Al-10Zn alloy in seawater was obtained by the different electrochemical technique such as (PDP and EIS). AFM was used to show the variations of the Cu-10Al-10Zn alloy corroded surface in solution before and after adding the inhibitor molecules.

Experimental

Synthesis of Inhibitors

In 250 mL round flask supply with a condenser and magnetic stirrer, 20 mM of different 1-bromo alkanes specifically, 1-bromo (hexane, dodecane, octadecane) were added separately to 20 mM of 5-methyl-1H-benzo[d][1,2,3]triazole. The acetone, 100 mL, was used as a solvent. The reaction mixture was refluxed at 70–80 ºC for about 36 h as shown in Scheme 1. Then cooled to the room temperature. The obtained pale brown precipitate product was further purified by diethyl ether. Then, recrystallized from acetone to give a pale brown precipitate of the cationic surfactants [14].

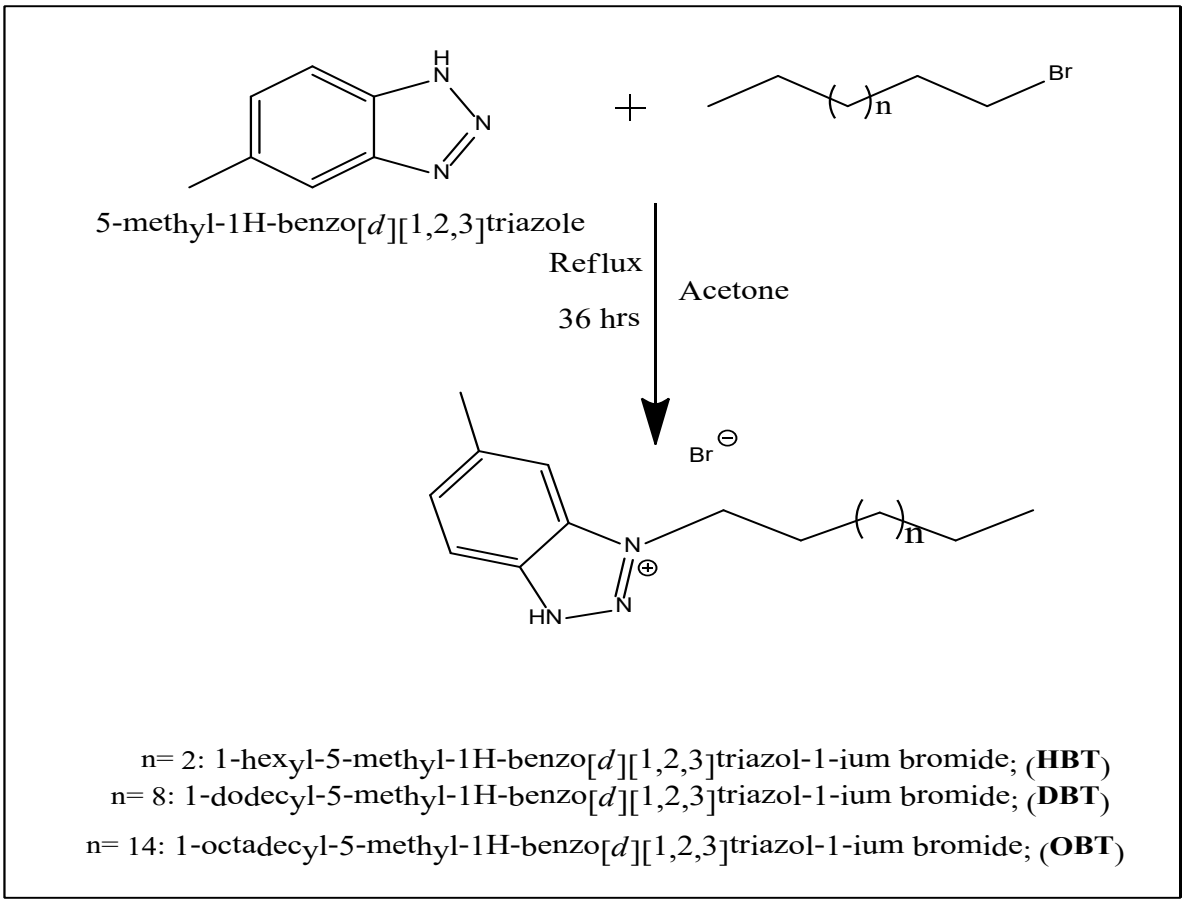

Scheme 1. The chemical structure of the prepared cationic surfactant.

Surface morphological observation

The analysis of the morphology of the Cu-10Al-10Zn alloy was carried out using atomic force microscopy (AFM) Wet – SPM with Non-Contact mode, in order to observe the change of the surface morphologies of the Cu-10Al-10Zn alloy after test in the media without and with addition of the inhibitor. Images of the specimens were recorded after two weeks exposure time in seawater at room temperature without and with (1.05×10^{-3} M) of inhibitor (OBT).

Electrochemical Measurements

Three-electrode system was used to evaluate the electrochemical performance of Cu-10Al-10Zn alloy in naturally aerated stagnant seawater solutions from the white mediterranean sea, which has chemical analysis as shown in Table 1 with the help of Volta lab potentiostat (Radiometer PGZ402) [5]. Saturated calomel electrode SCE, a platinum electrode as reference and counter electrodes respectively. The Cu-10Al-10Zn rod obtained by up casting procedure in metallurgical workshop and introduced into glass tubes by two-component epoxy resin leaving a surface area of 0.2 cm^2 to contact the solution. Metals analyzer (ARL 3460 OES) based on an average of three sparks per one specimen and tabulated in Table 2 detected the chemical composition of Cu-10Al-10Zn alloy. Electrochemical impedance spectroscopy was performed at steady state potential. EIS was carried out within frequency range (100000 - 0.05) HZ with amplitude 5 mV peak to peak. PDP was executed over sweeping potential range (-500 – 60) mV at scan rate (2) mV S^{-1}. Electrochemical impedance parameters have been fitted using Z_m view software by the suitable equivalent circuit. Before every measurement, the Cu-10Al-10Zn alloy polished by consecutive emery papers ranking from 600 to 2500 grit, then carefully washed with bi-distilled water and dried with soft paper, after that direct dipping in the corrosive medium. To obtain the desired concentration from the prepared inhibitors, a certain amount of inhibitor is dissolved into seawater. Series of solutions with lower concentrations were prepared by dilution. To verify reproducibility, every experiment was repeated at least three times.

TABLE (1): Complete chemical composition of seawater (as ions) used in this study.

Chemical composition	Na^+	Ca^{2+}	Mg^{2+} ions	Cl^-	SO_4^{2-}	HCO^{3-}	T.D.S.
Conc. / (g/L)	11.33	0.48	1.41	20.8	1.92	0.39	36.8

TABLE (2): Chemical composition of (Cu-10Al-10Zn) alloy used in this work.

Chemical composition	Cu	Al	Ni	Zn	Mn	Sn	Fe	Si	Mg
			Ti						
Conc. / (g/L)	79.14	10.40	0.00	10.20	0.01	0.02	0. 21	0.01	0.01	-------

Results and Discussion

Corrosion inhibitors characterization

The chemical structure of the as-synthesized surfactants in Scheme 1 was confirmed by FTIR and ^{1}HNMR spectra. Firstly, the FTIR spectrum shows the main characteristic bands of the prepared compound (HBT) as one of the prepared cationic compounds, presented in Fig.1. Where the absorption band appeared at 729.08 cm^{-1} is attributed to C-H bending out of the plan for the aromatic structure. The N-H stretch (secondary amine) appear at 3429 cm^{-1}, also, 3009 cm^{-1} is expected to C-H stretching in aromatic structure. 1624.80 cm^{-1} and 1468.08 cm^{-1} attributable to the C=C aromatic stretching of benzene. Typical bands, 2956-2862 cm^{-1} (aliphatic C-H stretching) [5]. The FTIR spectrum confirmed the predict function groups in the prepared compound. ^{1}HNMR spectrum of the prepared compound (HBT) is shown in Fig.2 [14]. The spectrum shows different bands at δ= 0.882 ppm (t, 3H, C***H***$_3$ $(CH_2)_3$ CH_2CH_2 N). Also δ=1.321 ppm (m, 6H, CH_3 $(CH_2)_3CH_2CH_2N$), δ= 1.65 ppm (m, 2H, CH_3 $(CH_2)_3CH_2CH_2N$), δ= 2.01 ppm (m, 2H, $CH_3(CH_2)_3CH_2CH_2N$), δ = 3.51ppm (s, 3H, C***H***$_3$-toluidene nucleus), δ=9.45 ppm (s,1H,N***H***) δ= 7.35 ppm (d, 1H, 4- benzene nucleus), δ= 7.84 (s, 1H, 6- benzene nucleus). The chemical composition of the synthesized cationic surfactants (HBT, DBT and OBT) (Scheme 1) was confirmed by elemental analysis using a Vario Elementar Analyzer (Hanau, Germany), (Table 3). The data of elemental analysis confirmed the purity of the synthesized inhibitors [15,16] .

TABLE (3): The elemental analysis of the prepared surfactants

Compound	*Structure*	*Yield, %*	*MWt (g/mol)*	*Carbon (C %)*		*Hydrogen (H %)*		*Nitrogen (N %)*		*Bromide (Br %)*	
				Calc.	***Found***	***Calc.***	***Found***	***Calc.***	***Found***	***Calc.***	***Found***
HBT	$C_{13}H_{20}N_3Br$	**71**	**298**	**52.36**	**52.23**	**6.76**	**6.69**	**14.09**	**14.02**	**26.79**	**26.63**
DBT	$C_{19}H_{32}N_3Br$	**82**	**382**	**59.68**	**59.57**	**8.44**	**8.37**	**10.99**	**10.89**	**20.9**	**20.81**
OBT	$C_{25}H_{44}N_3Br$	**85**	**466**	**64.36**	**64.24**	**9.51**	**9.43**	**9.01**	**8.92**	**17.13**	**17.02**

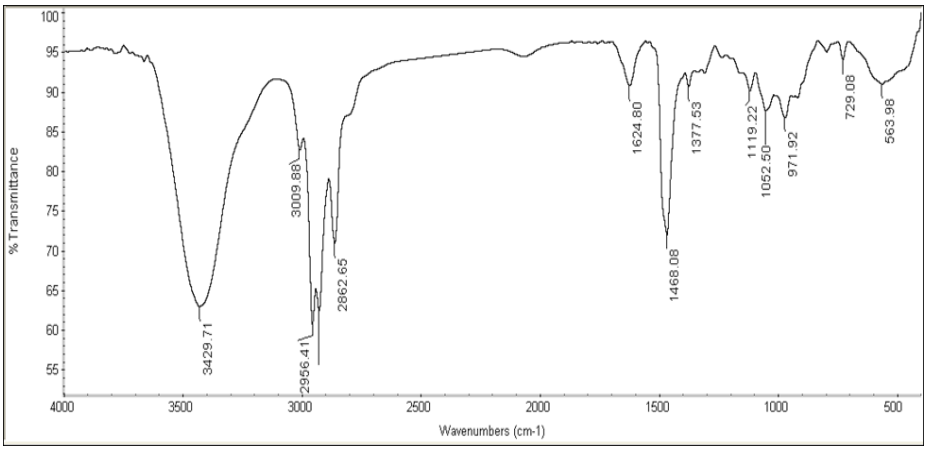

Fig. 1.FTIR spectrum of HBT.

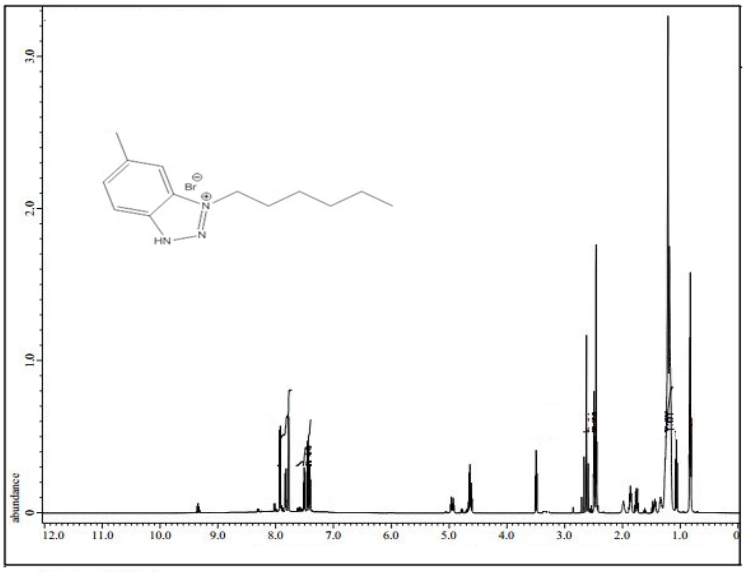

Fig. 2.^{1}H-NMR spectrum of HBT.

Polarization measurements

Potentiodynamic polarization technique is commonly used to study the phenomena of metal corrosion and passivation. The polarization technique was applied at a scan rate of 2 mV s^{-1} to determine both anodic and cathodic polarization curves for the corrosion of the Cu-10Al-10Zn alloy in seawater in absence and presence of the used inhibitor. Fig. 3(a, b, c) explained the effect of (HBT(6) DBT(12) OBT(18)) concentrations on cathodic and anodic polarization curves of Cu-10Al-10Zn alloy in seawater at 298 K. Parameters obtained from the polarization curves are shown in Table 4. This parameters including corrosion potentials (E_{corr}), corrosion current density (i_{corr}), corrosion rate (CR), cathodic and anodic tafel slope (βc, βa) respectively. Beside the inhibition efficiencies (η %), surface coverage and polarization resistance (R_p).The previous values can be calculated by using the following equations [17-21] :

η%=(1-i_corr/i_corr^°)×100 **(1)**

θ =(1-i_corr/i_corr^°) **(2)**

where (θ) represent the degree of the surface coverage, (i_corr^°, i_corr) represent the values of corrosion current density free and with inhibitor molecules, respectively. The well-known Stern–Geary equation was used to determine polarization resistance values (R_p):

R_p=b_a b_c/2.303 i_corr (b_a+b_c) **(3)**

Generally, the mechanisms of anodic dissolution of copper alloys, without inhibitor molecules, can be characterized via the following mechanism [22-24] :

$Cu \rightarrow Cu^{+} + e^{-}$ **(4)**

$Cu^{+} + Cl^{-} \rightarrow CuCl_{ads}$ **(5)**

$CuCl_{ads} + Cl^{-} \rightarrow CuCl^{-}_{2}$ **(6)**

Additional, the cathodic reaction that attain from reduction of oxygen in neutral or basic solution can be expressed by [22,25]:

$O_2 + 2H_2O + 4e^{-} \rightarrow 4OH^{-}$ **(7)**

By adding the inhibitor molecules, the corrosion rate of Cu-10Al-10Zn alloy has been decreased significantly, and hence moving the polarization curves directly toward lower current densities. The inhibition efficiencies results show the good inhibiting action of the prepared cationic surfactant. Furthermore, it can be seen that when the concentration of inhibitor increased, the inhibition efficiency increased reaching their maximum value, 94 %, at 1.05 x 10^{-3} M of OBT at 298 K as shown in Fig. 4 if we compare between the three compounds at the same concentration (1.05 x 10^{-3} M). Correspondingly, increasing in the carbon chain length of the prepared compounds provide a high inhibition performance for inhibitor OBT that indicate a full coverage of Cu-10Al-10Zn alloy surface with inhibitor molecules and lead to block the active anodic sites of metal surface by adsorbed inhibitor molecules, which lead to mitigate these active sites from reacting with the corrosive medium. On the other hand, the variability of tafel slopes (βa, βc) approved that cathodic and anodic reactions, oxygen reduction and metal dissolution, were affected without modifying the mechanism of corrosion [26]. There is no noticeable shift in corrosion potential values by adding the inhibitor molecules to both anodic and cathodic area and not exceed than 85 mV, there for the synthesized compounds categorized as mixed-type compounds [27-29]. Table.5 shows comparison between the η % of the prepared compound (OBT) and some other reported inhibitor for cu alloys in seawater [22,30,31].

TABLE (4): Polarization parameters and rates of corrosion of (Cu-10Al-10Zn) alloy in the absence and presence of different concentrations of different inhibitors in naturally aerated stagnant seawater at 298 K.

	Conc. (M x 10^{-3})	E_{corr} / mV_{SCE}	i_{corr} /mA cm^{-2}	β_a / mV dec^{-1}	B_c / mV dec^{-1}	Corr. rate / μmy^{-1}	Θ	R_p / $k\Omega$ cm^2	η%
	Blank	-291.2	0.0191	71.8	-245.3	222.6	_	2.30	_
HBT	0.13	-302.5	0.0125	63.8	-290.6	146.0	0.3455	2.83	34.55
	0.26	-314.9	0.00894	59.4	-316.4	104.2	0.5319	3.55	53.19
	0.52	-317.7	0.00651	50.8	-365.8	75.87	0.6592	3.93	65.92
	0.78	-337.9	0.00415	42.2	-428.2	48.36	0.7827	4.89	78.27
	1.05	-288.7	0.00216	31.6	-512.9	25.17	0.8869	6.76	88.69
DBT	0.13	-301.5	0.01077	65.1	-272	125.5	0.4361	2.30	43.61
	0.26	-275.7	0.00748	56.6	-326.9	87.11	0.6084	3.45	60.84
	0.52	-311	0.00553	45.5	-398.2	64.76	0.7105	3.97	71.05
	0.78	-363.6	0.0035	38.9	-466.6	40.76	0.8167	4.03	81.67
	1.05	-324.2	0.0016	25.3	-581.9	18.65	0.9162	5.26	91.62
OBT	0.13	-334.3	0.00924	60.2	-281.4	107.7	0.5162	2.30	51.62
	0.26	-319.4	0.00726	57.1	-375.7	84.65	0.6199	3.59	61.99
	0.52	-309.5	0.004353	46.5	-440.7	50.73	0.7749	4.02	77.49
	0.78	-274.3	0.00304	37.4	-553.9	35.45	0.8408	5.18	84.08
	1.05	-248.7	0.00102	19.6	-598.2	8.72	0.9466	5.72	94.66

TABLE (5): Comparison between the corrosion inhibition efficiency of the prepared (OBT) - cationic surfactant and some other reported inhibitor for copper alloys in saline water.

No	Inhibitor	Test medium	Optimum concentration	IE%	Test method	Reference
1	**OBT**	**Seawater**	1.05×10^{-3} (M) (400 ppm)	94.66	PDP	Present study
2	**TTA (24)**		400 ppm	90	PDP	[22]
3	**Purine**		5×10^{-3} (M)	91.91	PDP	[30]
4	**Imidazole**		5×10^{-3} (M)	84.35	PDP	[30]
5	**(AMLA)**		1000 ppm	79.99	EIS	[31]

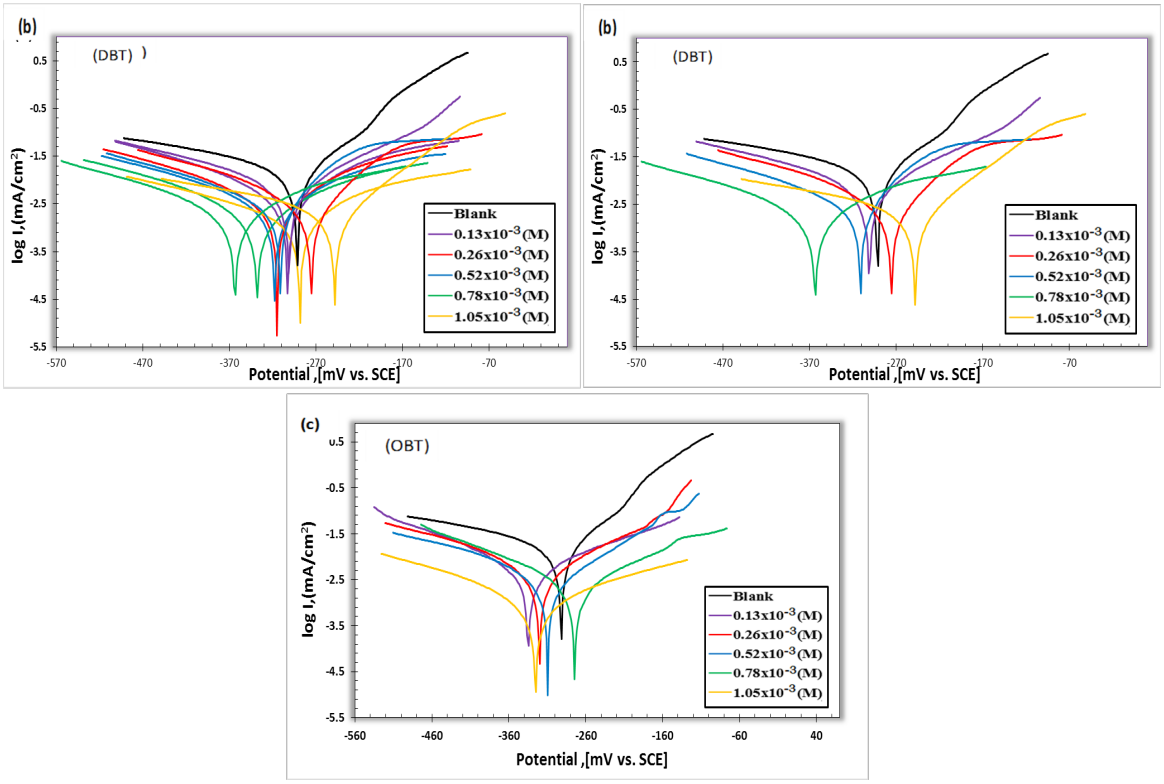

Fig. 3. Polarization curves of (Cu-10Al-10Zn) alloy in seawater without and with various concentrations of inhibitor at 298 K: HBT (a), DBT (b) and OBT (c).

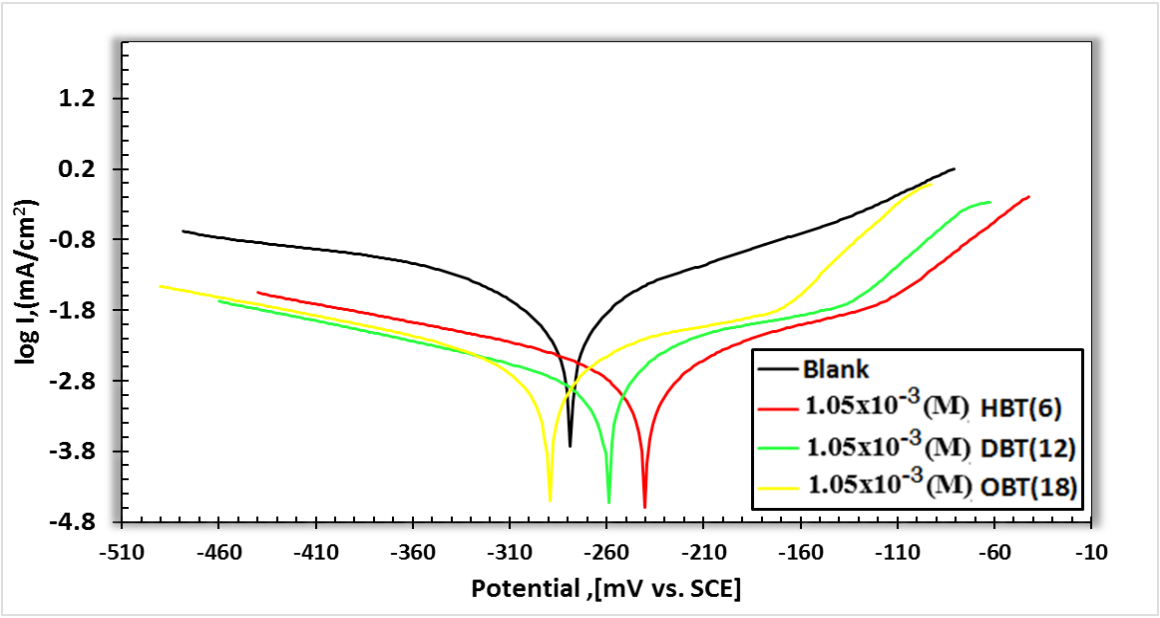

Fig. 4. Potentiodynamic polarization curves of the (Cu-10Al-10Zn) alloy after electrode immersion in stagnant naturally aerated seawater free and containing (1.05 x 10^{-3} M) of the different inhibitors at 298 K.

The electrochemical impedance spectroscopy measurements

Corrosion behavior of Cu-10Al-10Zn alloy in seawater without and with different concentrations of the synthesized three-benzotriazole cationic surfactants (HBT, DBT and OBT) was studied by EIS technique. Fig. 5(a–c) and Fig. 6(a–c) shows the typical Nyquist and Bode plots for the Cu-10Al-10Zn alloy at the various concentrations of the three prepared surfactants. From the obtained Nyquist and Bode plots, it was observed that, the impedance response of Cu-10Al-10Zn alloy in the corrosive medium directly changed after the addition of surfactant molecules. A suitable equivalent circuit (EC) model presented in Fig.7 analyzed the impedance data of the prepared surfactants by using EIS analyzer software program. Moreover, the calculated equivalent circuit parameters at different inhibitor concentration including, film resistance, solution resistance, film capacitance and double layer capacitance are presented in Table 6. The electrochemical impedance parameters such as the charge transfer resistance and percentage inhibition efficiency were calculated and listed in Table 6. The following equation can be used to calculate the values of inhibition efficiency from values {Bayol, 2008 #2364} [32-34]:

$$\eta\% = (1 - R\_ct(uninh) / R\_ct(inh)) \times 100 \quad \textbf{(8)}$$

where and are the charge transfer resistance values in the absence and presence of inhibitor molecules, respectively. The diameter of the Nyquist plots, Fig. 5(a–c), showed that the recorded impedance values (real resistance (Z_r)) increased by increasing the inhibitor concentration comparatively to the blank solution indicating that the alloy surface gets more protection. It is clear also that from the obtained Nyquist plots, two badly separated depressed capacitive loops exhibited, this depressed behavior is due to the frequency dispersion [35]. From Fig. 6(a–c) and data presented in table 6, it was observed that, value of inhibitor (OBT) is greater than that of inhibitors ((HBT), (DBT)) thereby, indicating higher inhibition efficiency of inhibitor (OBT) than the other two inhibitors. Also the values of are decreased gradually by the addition of the prepared cationic surfactants compared to values of the blank solution. Increasing the charge transfer resistance values and decreasing the electrochemical double layer capacitance of the tested inhibitors by increasing the inhibitor concentration was attributed to replacement of the water molecules in the double layer by the adsorbed inhibitor molecules which form adherent protective film on the alloy surface and increasing in the surface coverage of the Cu-10Al-10Zn alloy [36]. The band of impedance is described by two capacitive loops or two-phase maxima [37].The first phase maxima, one small loop, exists at high

frequency area and caused by the double layer capacitance as a result of adsorption of surfactant molecules at the surface of the Cu-10Al-10Zn alloy. The last phase maxima, large incomplete capacitive loop, exist at low-frequency area and controlled by the film formation. This film changes the structure at the electrode/solution interface [38]. The Bode curves of Cu-10Al-10Zn alloy in seawater without and with different concentrations of the prepared surfactants, Fig. 6(a–c), indicate that there is a significant increase in the impedance value by increasing the inhibitors concentration in the solution, which increase the surface coverage of the alloy and exhibit a high inhibition performance [39]. The order of obtained for the R_{ct} values was in the following order (OBT> DBT> HBT). Thereby, agree with above-mentioned results for the potentiodynamic polarization measurements. The variation in the statues of Cu-10Al-10Zn alloy in both of tafel and EIS techniques is a major reason for changing in efficiency values [40,41] .

TABLE (6): Electrochemical impedance spectroscopy (EIS) parameters of (Cu-10Al-10Zn) alloy in naturally aerated stagnant seawater in the absence and presence of different concentrations of HBT, DBT and OBT at 298 K.

Inhibitor	*Conc.* (*M x 10⁻³*)	R_s (Ω cm^2)	C_f (μF.cm^{-2}) *10^{-5}	n_1	R_f (Ω cm^2)	C_{dl} (μF.cm^{-2})*10^{-3}	n_2	R_{ct} (kΩ cm^2)	*IE%*
Blank	---	4.0343	22.31	0.8794	90.65	5.623	0.8027	1.02	---
HBT	0.13	4.6813	4.120	0.8851	187.3	1.034	0.8256	2.01	49.25
	0.26	4.2346	3.979	0.8487	188.9	0.592	0.7385	2.6	60.76
	0.52	6.3671	4.009	0.8	224.2	0.126	0.7980	2.91	64.94
	0.78	6.7472	3.243	0.7521	239.4	0.121	0.8170	4.45	77.07
	1.05	3.1392	3.445	0.8041	276.9	0.112	0.8	5.5	81.45
DBT	0.13	4.8269	4.063	0.8002	126.1	0.723	0.8769	2.31	55.84
	0.26	3.2071	3.546	0.8301	192.5	0.375	0.8429	3.10	67.09
	0.52	3.2468	3.179	0.8641	287.6	0.196	0.8467	3.51	70.94
	0.78	3.1705	2.765	0.8	291.4	0.102`	0.7584	4.56	77.63
	1.05	3.0996	3.842	0.7981	304.3	0.109	0.8	5.99	82.97
OBT	0.13	4.2431	4.892	0.8689	118.9	0.482	0.8	2.56	60.15
	0.26	6.2945	3.925	0.8919	253.7	0.251	0.7672	2.91	64.94
	0.52	3.7824	3.458	0.8988	472.6	0.183	0.8965	3.66	72.13
	0.78	6.2792	3.632	0.8940	309.1	0.112	0.7261	4.75	78.52
	1.05	3.6959	3.224	0.8988	364.1	0.103	0.8999	7.31	86.04

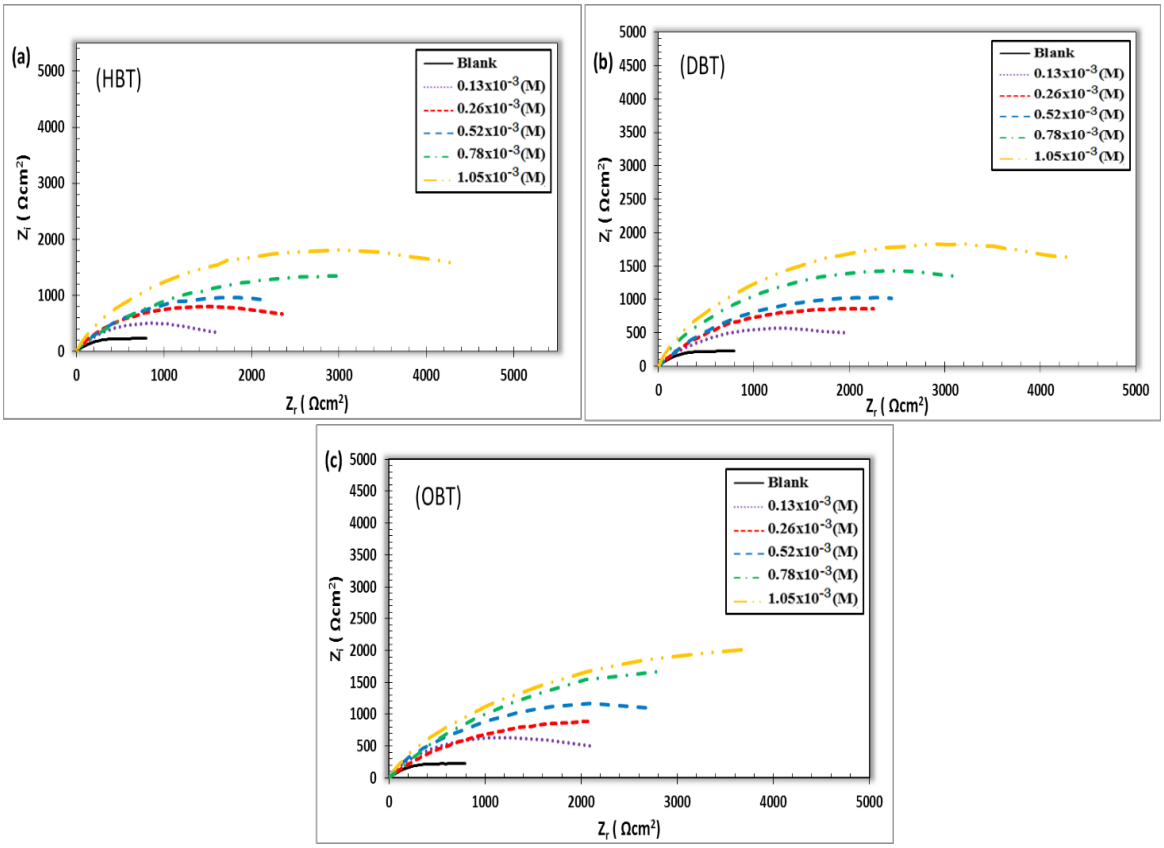

Fig.5 Nyquist plot of (Cu-10Al-10Zn) alloy in seawater with different concentrations of (a) HBT, (b) DBT and (c) OBT

Adsorption isotherm

To attain more information about the interaction between the inhibitor molecules with Cu-10Al-10Zn alloy surface, different adsorption isotherms were tested such as langmuir, Temkin, Freundlich and Flory-Huggines adsorption isotherms as listed in the supplementary data that were shown in **Fig. S (1, 2and 3)** respectively. Moreover, the best fitted molecule was Langmuir adsorption isotherm due to highly R^2 and unity of slop [42-44]. From the electrochemical polarization technique at different concentrations we can calculate the degree of surface coverage () according to [45] :

$$\Theta=(i\_corr-i\_(corr(inh))/i\_corr\ ) \quad (9)$$

The relation between surface coverage area () and the inhibitor concentration () is given by Langmuir model through the following equation [46,47] .

$$C\_inh/\Theta=1/K\_ads+C\_inh \quad (10)$$

where is the degree of surface coverage obtained from (DC) polarization measurements, is the molar concentration of the prepared inhibitors and is the standard adsorption equilibrium constant. The relation between and was used to get the best fitting adsorption isotherm. Fig.8 explains Langmuir adsorption isotherm of the three inhibitors on the surface of Cu-10Al-10Zn alloy in seawater at 298 K. A straight line was obtained on plotting against with a regression coefficient (r^2) values; 0.9898, 0.99 and 0.9911 for HBT, DBT and OBT, respectively and with slops, Table 7, close to unity indicating that the adsorption of each inhibitor on Cu-10Al-10Zn alloy surface completely followed this isotherm. The equilibrium constant values (were calculated from the intercept of the straight line. The equilibrium constant values (is related to the standard free energy of adsorption, with the following equation [48,49] .

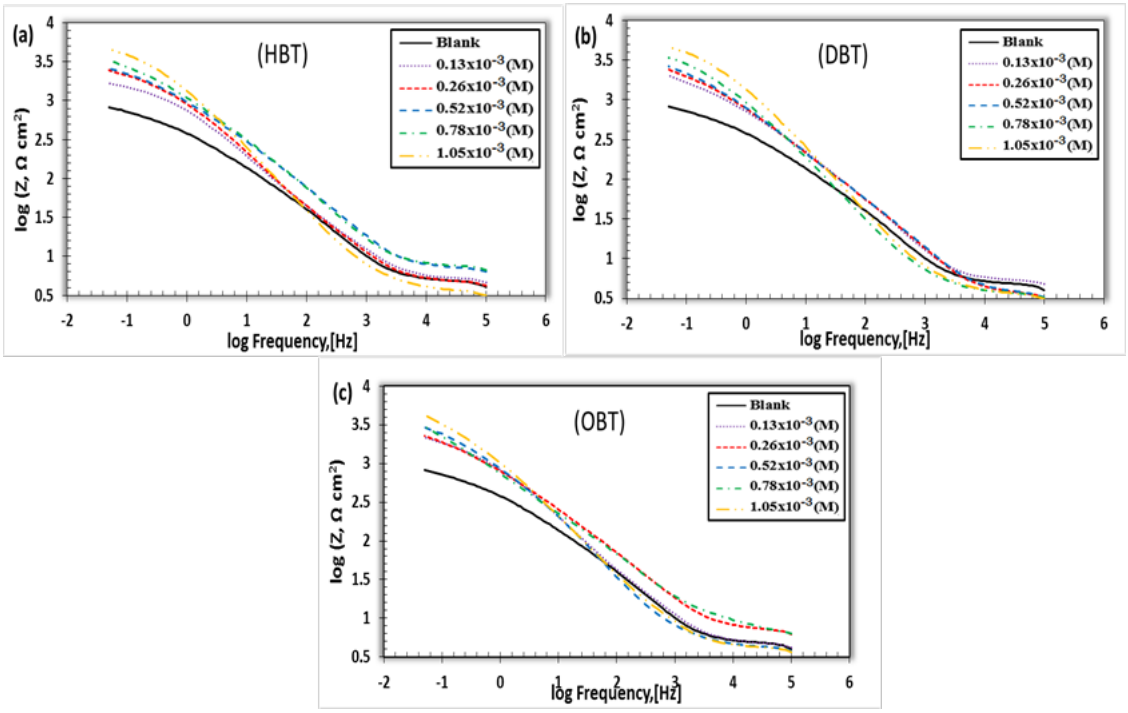

Fig.6 Bode plot of (Cu-10Al-10Zn) alloy in seawater with different concentrations of (a) HBT, (b) DBT and (c) OBT.

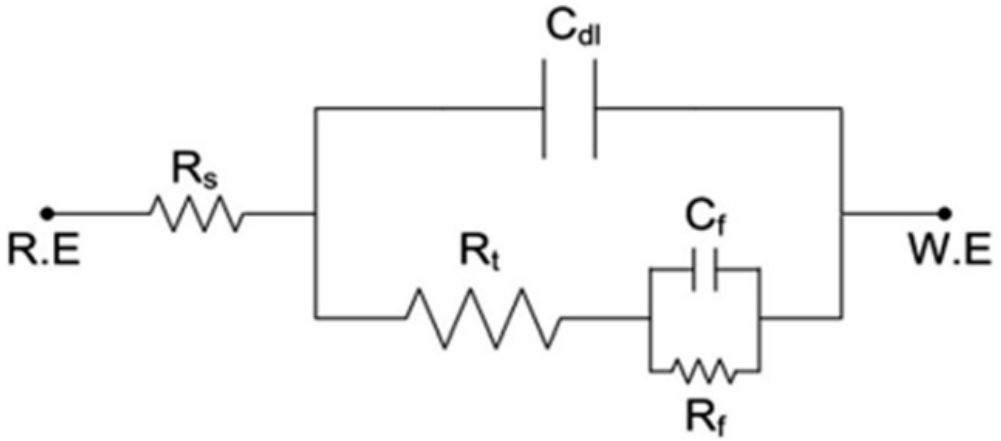

Fig. 7. Equivalent circuit (EC) used to simulate impedance data for (Cu-10Al-10Zn) alloy in seawater.

$$\Delta G^{\circ}_{ads} = -RT \ln (55.5K_{ads}) \quad \textbf{(11)}$$

where *R*, (8.314 J /mol.K), is the universal gas constant, *T* is the absolute temperature. The (55.5) value associated to the molar concentration of water expressed in mol/L [50]. The calculated values of for all prepared inhibitors are recorded in Table 7. The negative sign of detect that all the prepared inhibitor molecules are spontaneously adsorbed onto the Cu-10Al-10Zn alloy surface. It is reported in the literature that, if the absolute value of at -20 kJ/mol or less negative indicates that the adsorption of inhibitor molecules on the Cu-10Al-10Zn alloy surface attributed to the electrostatic interaction between the positive and negative charges located in the quaternary nitrogen and adsorbed chloride on the Cu-10Al-10Zn alloy surface correspondingly i.e. physisorption. On the other hand, if the value of at -40 kJ/mol or more negative, it functions by chemical adsorption as a result of a charge transfer from the inhibitor molecule to the Cu-10Al-10Zn alloy surface [27,51]. From Table 7 the calculated values of indicated that the adsorption of the prepared cationic surfactant on the surface of Cu-10Al-10Zn alloy in seawater is of a mixed type (physical and chemical) adsorption. It was noticed that, the value of for adsorbed OBT on Cu-10Al-10Zn alloy surface is higher than that of HBT or DBT. This indicates that OBT is more effective, enhanced more inhibition efficiency. Therefore, these results are in good agreement with the experimental data. From this prospective, we suggest that the inhibition mechanism maybe followed according to Fig.9, in which physical adsorption involves electrostatic interaction between the positive quaternary nitrogen on the inhibitor molecules and the negative adsorbed chloride on the Cu-10Al-10Zn alloy surface. In addition, adsorption of bromide ion on positively charged Cu-10Al-10Zn alloy surface that enhanced\synergized the probability of the adsorption process and making a protective layer on the Cu-10Al-10Zn alloy surface. Additionally, chemisorption implicates charge sharing or charge transfer to form a coordinate covalent bond between the Cu-10Al-10Zn alloy surface and adsorbed prepared inhibitor molecules. The non-polar carbon-chain has high electron density that keeps the aggressive chloride anions away from the Cu-10Al-10Zn alloy surface. Thus, this enhance the adsorption property of the synthesized compounds on Cu-10Al-10Zn alloy surface.

TABLE (7): Thermodynamic parameter for adsorption of the prepared inhibitor for (Cu-10Al-10Zn) alloy in seawater at 298 K.

Inhibitor	Slope	Regression coefficient (r^2)	K_{ads} (M^{-1})	$\Delta G^{\circ}ads$ (kJ/mol)
(HBT)	1.0237	0.9898	3333.333	-30.05
(DBT)	0.9809	0.99	5000	-31.05
(OBT)	0.9980	0.9911	10000	-32.77

(AFM) surface characterization

To obtain the change of the surface morphologies of the Cu-10Al-10Zn alloy after test in the media without and with addition of the inhibitor molecules. Images of the specimens were recorded after (15 days) exposure time in seawater at room temperature without and with (1.05 x 10^{-3} M) of (OBT) inhibitor. Fig.10 (a, b) shows the surface morphology (3D) of the sample after exposure to seawater solution in absence and presence of 1.05 x 10^{-3} M of OBT inhibitor.

Fig.10 (a) shows a rough surface of Cu-10Al-10Zn alloy without adding the inhibitor, which strongly damaged because of the dissolution of the metals in the corrosive solution. Also, the presence of 1.05 x 10^{-3} M of OBT inhibitor molecule for identical time (15 days) give smooth and less damaged surface as shown in Fig.10 (b) . The value of surface roughness, derived from (AFM) height profile images, (Fig.10), for the Cu-10Al-10Zn alloy in the absence of inhibitor and after exposure to seawater is (4.71) µm. While

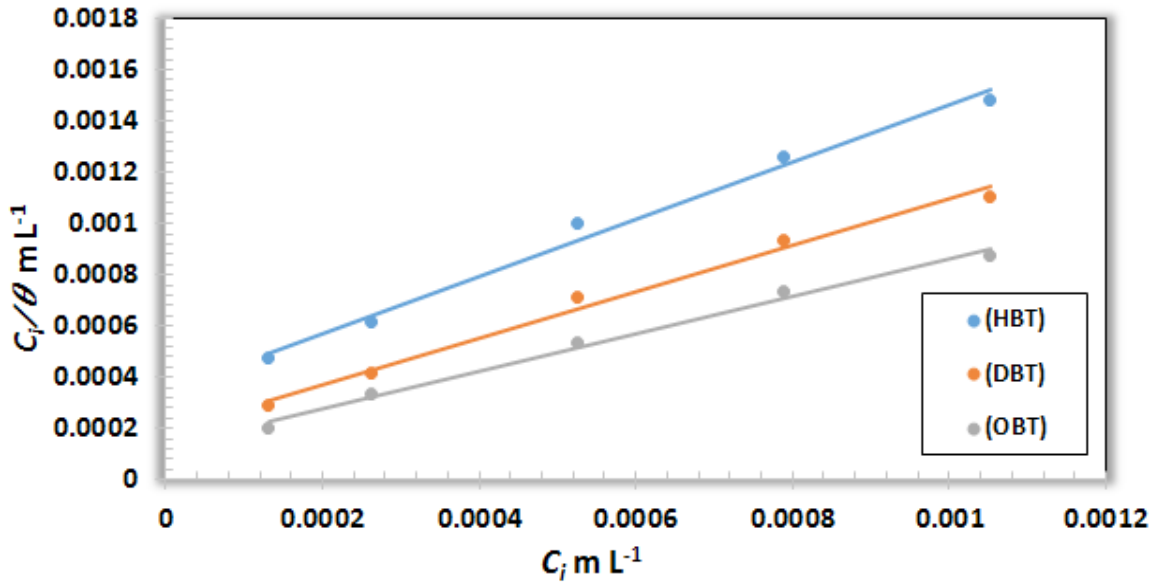

Fig. 8 Langmuir adsorption isotherm curve (Ci/θ vs. Ci) for the prepared inhibitors on the surface of Cu-10Al-10Zn alloy in seawater at 298 K.

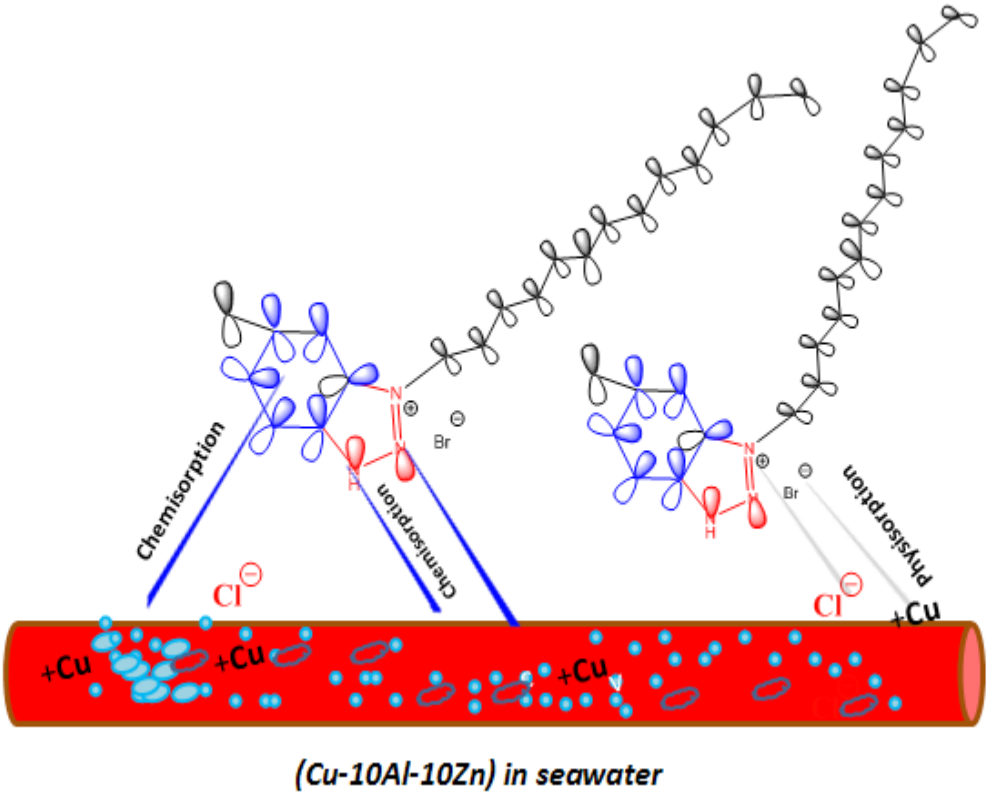

Fig. 9 Illustration of the adsorption behaviour of the prepared inhibitor.

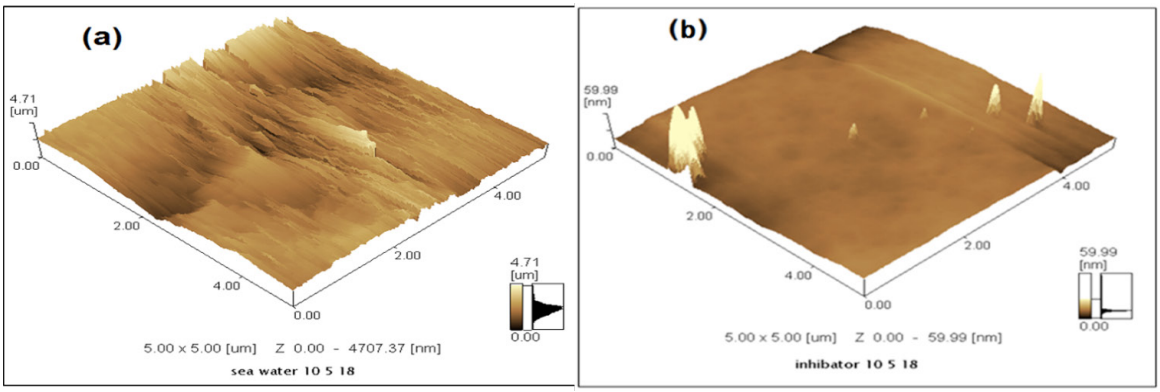

Fig.10 AFM Micrographs of Cu-10Al-10Zn alloy surface (a) in seawater, (b) in presence of (1.05 x 10-3 M) of (OBT).

in the existence of 1.05 x 10^{-3} M of OBT inhibitor decreased to (59.99) nm. Decreasing in roughness attributed to the protection film being absorbed on the Cu-10Al-10Zn alloy surface. This film of inhibitor molecules was adherent to the surface which leads to a high level of inhibition efficiency. The results of obtained AFM are well correlated with the previous electrochemical measurements {El Wanees, 2017 #2400} {Abd El Wanees, 2017 #2399} [52-54].

Conclusions

Three prepared cationic surfactants have been investigated for their inhibition efficiency for corrosion of Cu-10Al-10Zn alloy in seawater. The results indicated that, all prepared inhibitors could inhibit Cu-10Al-10Zn alloy corrosion in seawater and their corrosion inhibition efficiencies increased by increasing the inhibitor concentration. Adsorption of the inhibitor molecules mainly attributed to a physico-chemical adsorption, as was confirmed from the calculated standard Gibbs free energy values obtained from Langmuir adsorption model. The DC polarization curves designated that the inhibitor molecules act as mixed type inhibitors, which impede the dissolution of the metal (anodic) besides oxygen reduction (cathodic). EIS data revealed that the values of increased and values are decreased progressively via increasing the concentration of the inhibitor molecules compared to values of the blank solution. Both of Potentiodynamic polarization and electrochemical impedance technique show that, the (η %) value of inhibitor (OBT) is higher than that of inhibitors (HBT and DBT). AFM analysis shows a smother surface of alloy after adding the inhibitor molecule, which confirms the formation of a protective film on the Cu-10Al-10Zn alloy surface, preventing it from direct contact with corrosive ions.

Acknowledgement

Special thanks to the Egyptian Petroleum Research Institute (EPRI) for their support to the laboratories.

References

1. Drach A., Tsukrov I., DeCew J., Aufrecht J., Grohbauer A. and Hofmann U., Field studies of corrosion behaviour of copper alloys in natural seawater. *Corrosion science*, **76** 453-464(2013).

2. El Warraky A., El Shayeb H. and Sherif E., Pitting corrosion of copper in chloride solutions. *Anti-Corrosion Methods and Materials*, **51**(1), 52-61(2004).

3. Qiu L.-G., Xie A.-J. and Shen Y.-H., The adsorption and corrosion inhibition of some cationic gemini surfactants on carbon steel surface in hydrochloric acid. *Corrosion Science*, **47**(1), 273-278(2005).

4. Elgendy A., Elkholy A.E., El Basiony N.M. and Migahed M.A., Monte Carlo simulation for the antiscaling performance of Gemini ionic liquids. *Journal of Molecular Liquids*, **285** 408-415(2019).

5. Migahed M., El-Rabiei M., Nady H. and Fathy M., Synthesis, characterization of some ethoxylated tolyltriazole derivatives and evaluation of their performance as corrosion inhibitors for Cu-10Al

alloy in seawater. *Journal of Environmental Chemical Engineering*, **4**(4), 3741-3752(2016).

6. Popova A., Christov M. and Vasilev A., Inhibitive properties of quaternary ammonium bromides of N-containing heterocycles on acid mild steel corrosion. Part II: EIS results. *Corrosion Science*, **49**(8), 3290-3302(2007).

7. Sherif E.-S.M., Erasmus R. and Comins J., Corrosion of copper in aerated synthetic sea water solutions and its inhibition by 3-amino-1, 2, 4-triazole. *Journal of colloid and interface science*, **309**(2), 470-477(2007).

8. Sharma V., Borse M., Jauhari S., Pai K. and Devi S., New hydroxylated cationic gemini surfactants as effective corrosion inhibitors for mild steel in hydrochloric acid medium. *Tenside Surfactants Detergents*, **42**(3), 163-167(2005).

9. Hussien B., Al-Sabagh A., Migahed M., Shaban M. and Moawad Z., Corrosion Control of X-60 Type Carbon Steel in Petroleum Formation Water Under High Pressure of CO2 at High Temperature, Offshore Mediterranean Conference and Exhibition, Offshore Mediterranean Conference, 2017.

10. Finšgar M. and Milošev I., Inhibition of copper corrosion by 1, 2, 3-benzotriazole: a review. *Corrosion science*, **52**(9), 2737-2749(2010).

11. Hussien B., Migahed M., Shaban M., Negm N. and Moawad Z., Synthesis and Inhibition Performance of Diquaternary Ammonium Gemini Surfactants on Carbon Steel Pipelines Corrosion in Gas Field, Offshore Mediterranean Conference and Exhibition, Offshore Mediterranean Conference, 2017.

12. Wang Z., Gong Y., Jing C., Huang H., Li H., Zhang S. and Gao F., Synthesis of dibenzotriazole derivatives bearing alkylene linkers as corrosion inhibitors for copper in sodium chloride solution: A new thought for the design of organic inhibitors. *Corrosion Science*, **113** 64-77(2016).

13. Ravichandran R., Nanjundan S. and Rajendran N., Effect of benzotriazole derivatives on the corrosion of brass in NaCl solutions. *Applied Surface Science*, **236**(1-4), 241-250(2004).

14. Hegazy M., Novel cationic surfactant based on triazole as a corrosion inhibitor for carbon steel in phosphoric acid produced by dihydrate wet process. *Journal of Molecular Liquids*, **208** 227-236(2015).

15. Zaky M., Badawi A., Ead H. and Aboulimoud M., Novel Cationic Schiff Base Surfactants: Surface Studies and Biocidal Activities against Bacteria Fungi and Sulfate Reducing Bacteria. DOI

16. Negm N.A., Zaki M.F. and Salem M.A., Synthesis and evaluation of 4-diethyl amino benzaldehyde Schiff base cationic amphiphiles as corrosion inhibitors for carbon steel in different acidic media. *Journal of surfactants and detergents*, **12**(4), 321-329(2009).

17. Bayol E., Gürten T., Gürten A.A. and Erbil M., Interactions of some Schiff base compounds with mild steel surface in hydrochloric acid solution. *Materials Chemistry and Physics*, **112**(2), 624-630(2008).

18. Zhang Q. and Hua Y., Corrosion inhibition of mild steel by alkylimidazolium ionic liquids in hydrochloric acid. *Electrochimica Acta*, **54**(6), 1881-1887(2009).

19. Radwan A.B., Sliem M.H., Okonkwo P.C., Shibl M.F. and Abdullah A.M., Corrosion inhibition of API X120 steel in a highly aggressive medium using stearamidopropyl dimethylamine. *Journal of Molecular Liquids*, **236** 220-231(2017).

20. Abdelaal M.M., Mohamed S.G., Barakat Y.F., AY H., Derbala H.H. and Al Zoubi W., N-aminophthalimide as a Synthon for Heterocyclic Schiff bases: Efficient Utilization as Corrosion Inhibitors of Mild Steel in 0.5 mol. L-1 H2SO4 Solution. DOI (2017).

21. Migahed M., El-Shafei A., Fouda A. and Morsi M., Corrosion Inhibition of Carbon Steel in Hydrochloric Acid Solution Using Barbituric Acid and its Substituted. DOI

22. Nady H., El-Rabiei M., Migahed M. and Fathy M., Corrosion Control of Cu-10Al-10Ni and Cu-10Al-10Zn Alloys in Seawater Environment by Some Ethoxylated Tolyltriazole Derivatives. *Zeitschrift für Physikalische Chemie*, **231**(6), 1179-1209(2017).

23. Lee H. and Nobe K., Kinetics and mechanisms of Cu electrodissolution in chloride media. *Journal of the Electrochemical Society*, **133**(10), 2035-2043(1986).

24. Barcia O., Mattos O., Pebere N. and Tribollet B., Mass-transport study for the electrodissolution of copper in 1M hydrochloric acid solution by impedance. *Journal of the Electrochemical Society*, **140**(10), 2825-2832(1993).

25. Kear G., Barker B., Stokes K. and Walsh F., Electrochemical corrosion behaviour of 90—10

Cu—Ni alloy in chloride-based electrolytes. *Journal of Applied Electrochemistry*, **34**(7), 659-669(2004).

26. Migahed M., Attia A. and Habib R., Study on the efficiency of some amine derivatives as corrosion and scale inhibitors in cooling water systems. *RSC Advances*, **5**(71), 57254-57262(2015).

27. Migahed M., EL-Rabiei M., Nady H. and Zaki E., Novel Gemini cationic surfactants as anti-corrosion for X-65 steel dissolution in oilfield produced water under sweet conditions: Combined experimental and computational investigations. *Journal of Molecular Structure*, **1159** 10-22(2018).

28. El Basiony N.M., Elgendy A., Nady H., Migahed M.A. and Zaki E.G., Adsorption characteristics and inhibition effect of two Schiff base compounds on corrosion of mild steel in 0.5 M HCl solution: experimental, DFT studies, and Monte Carlo simulation. *RSC Advances*, **9**(19), 10473-10485(2019).

29. Migahed M.A., elgendy A., El-Rabiei M.M., Nady H. and Zaki E.G., Novel Gemini cationic surfactants as anti-corrosion for X-65 steel dissolution in oilfield produced water under sweet conditions: Combined experimental and computational investigations. *Journal of Molecular Structure*, **1159** 10-22(2018).

30. Mihajlović M.B.P., Radovanović M.B., Tasić Ž.Z. and Antonijević M.M., Imidazole based compounds as copper corrosion inhibitors in seawater. *Journal of Molecular Liquids*, **225** 127-136(2017).

31. Fateh A., Aliofkhazraei M. and Rezvanian A., Review of corrosive environments for copper and its corrosion inhibitors. *Arabian journal of Chemistry*, DOI (2017).

32. Biswas A., Pal S. and Udayabhanu G., Experimental and theoretical studies of xanthan gum and its graft co-polymer as corrosion inhibitor for mild steel in 15% HCl. *Applied Surface Science*, **353** 173-183(2015).

33. Gopi D., Govindaraju K., Prakash V.C.A., Sakila D.A. and Kavitha L., A study on new benzotriazole derivatives as inhibitors on copper corrosion in ground water. *Corrosion Science*, **51**(10), 2259-2265(2009).

34. Yadav A., Nishikata A. and Tsuru T., Electrochemical impedance study on galvanized steel corrosion under cyclic wet–dry conditions—influence of time of wetness. *Corrosion Science*, **46**(1), 169-181(2004).

35. Al-Sabagh A., Migahed M., Sadeek S. and El Basiony N., Inhibition of mild steel corrosion and calcium sulfate formation in highly saline synthetic water by a newly synthesized anionic carboxylated surfactant. *Egyptian journal of petroleum*, **27**(4), 811-821(2018).

36. Emregül K.C. and Atakol O., Corrosion inhibition of iron in 1 M HCl solution with Schiff base compounds and derivatives. *Materials Chemistry and Physics*, **83**(2-3), 373-379(2004).

37. Frignani A., Grassi V., Zanotto F. and Zucchi F., Inhibition of AZ31 Mg alloy corrosion by anionic surfactants. *Corrosion Science*, **63** 29-39(2012).

38. Farsak M., Keleş H. and Keleş M., A new corrosion inhibitor for protection of low carbon steel in HCl solution. *Corrosion Science*, **98** 223-232(2015).

39. Negm N., Migahed M., Farag R., Fadda A., Awad M. and Shaban M., High performance corrosion inhibition of novel tricationic surfactants on carbon steel in formation water: Electrochemical and computational evaluations. *Journal of Molecular Liquids*, **262** 363-375(2018).

40. Hosseini M., Ehteshamzadeh M. and Shahrabi T., Protection of mild steel corrosion with Schiff bases in 0.5 M H2SO4 solution. *Electrochimica acta*, **52**(11), 3680-3685(2007).

41. 41. Migahed M., EL-Rabiei M., Nady H., Elgendy A., Zaki E., Abdou M. and Noamy E., Novel ionic liquid compound act as sweet corrosion inhibitors for X-65 carbon tubing steel: experimental and theoretical studies. *Journal of Bio-and Tribo-Corrosion*, **3**(3), 31(2017).

42. Damaskin B.B., Petrii O.A. and Batrakov V.V., Adsorption of organic compounds on electrodes. DOI (1971).

43. Lipkowski J. and Ross P.N., Adsorption of molecules at metal electrodes, VCH New York1992.

44. Stupnišek-Lisac E., Gazivoda A. and Madžarac M., Evaluation of non-toxic corrosion inhibitors for copper in sulphuric acid. *Electrochimica acta*, **47**(26), 4189-4194(2002).

45. Helal N. and Badawy W., Environmentally safe corrosion inhibition of Mg–Al–Zn alloy in chloride free neutral solutions by amino acids. *Electrochimica Acta*, **56**(19), 6581-6587(2011).

46. Başar C.A., Applicability of the various adsorption models of three dyes adsorption onto activated carbon prepared waste apricot. *Journal of*

Hazardous Materials, **135**(1-3), 232-241(2006).

47. Ismail M., Megahed H., Ali A.I. and El-Etre M.A., Application of theophylline anhydrous as inhibitor for acid corrosion of aluminum. *Egypt. J. Chem*, **60**(1), 95-107(2017).

48. Martinez S. and Stern I., Thermodynamic characterization of metal dissolution and inhibitor adsorption processes in the low carbon steel/ mimosa tannin/sulfuric acid system. *Applied Surface Science*, **199**(1-4), 83-89(2002).

49. Zaky M.F., Sabbah I., Negm N.A. and Hendawy M., Biocidal Activity and Corrosion Inhibition of Some Cationic Surfactants Derived from Thiol Polyurethane. *Egyptian Journal of Chemistry*, **61**(1), 45-60(2018).

50. Wang X., Yang H. and Wang F., A cationic gemini-surfactant as effective inhibitor for mild steel in HCl solutions. *Corrosion Science*, **52**(4), 1268-1276(2010).

51. Kannan P., Karthikeyan J., Murugan P., Rao T.S. and Rajendran N., Corrosion inhibition effect of novel methyl benzimidazolium ionic liquid for carbon steel in HCl medium. *Journal of Molecular Liquids*, **221** 368-380(2016).

52. Yurt A., Duran B. and Dal H., An experimental and theoretical investigation on adsorption properties of some diphenolic Schiff bases as corrosion inhibitors at acidic solution/mild steel interface. *Arabian Journal of Chemistry*, **7**(5), 732-740(2014).

53. El Wanees S.A., ElBasiony N., Al-Sabagh A., Alsharif M., El Haleem S.A. and Migahed M., Controlling of H2 gas production during Zn dissolution in HCl solutions. *Journal of Molecular Liquids*, **248** 943-952(2017).

54. Abd-Elaal A.A., Elbasiony N., Shaban S.M. and Zaki E., Studying the corrosion inhibition of some prepared nonionic surfactants based on 3-(4-hydroxyphenyl) propanoic acid and estimating the influence of silver nanoparticles on the surface parameters. *Journal of Molecular Liquids*, **249** 304-317(2018).

السلوك الكهروكيميائى لسبيكة النحاس-الألومنيوم-الزنك في مياه البحر في غياب وفى وجود مركبات البنزوتريازول الكاتيونية

محمد عطية مجاهد [أ]، احمد ناصر [ب]، هشام الفقي [ج]، محمد الربيعي [ج]
[أ]معهد بحوث البترول، مدينة نصر، القاهرة،.,[ب] المعهد العالي للهندسة والتكنولوجيا الحديثة ، المرج، القليوبية، , [ج] قسم الكيمياء، كلية العلوم، جامعة الفيوم- مصر.

تمت دراسة سلوك سبيكة النحاس-الألومنيوم-الزنك في مياه البحر في غياب وفى وجود تراكيز مختلفة من المواد ذات النشاط السطحي وهي: -

- (1-hexyl-5-methyl-1H-benzo[d] [1, 2, 3] triazole-1-ium bromid (HBT (6)).
- (1-dodecyl-5-methyl-1H-benzo[d] [1, 2, 3] triazole-1-ium bromid (DBT (12)).
- (1-octadecyl-5-methyl-1H-benzo[d] [1, 2, 3] triazole-1-ium bromid (OBT (18)).

كمثبطات للتأكل. وقد تم إثبات التركيب الكيميائي لهذه المركبات بعد تحضيرها، (HBT) كمركب تمثيلي، عن طريق FT-IR و ^{1}H-NMR. وتم استخدام التقنيات الكهروكيميائية التقليدية مثل طرق قياس الاستقطاب الخطى (DC) والمعاوقة الكهروكيميائية (EIS). وقد أوضحت النتائج التي تم الحصول عليها ان قيم الكفاءة تزداد بزيادة تركيز المثبط في المحلول. وأظهرت منحنيات الاستقطاب الخطى (DC) والمعاوقة الكهروكيميائية (EIS) أن أداء جميع المركبات المحضرة من النوع المختلط. وتشير قيم الطاقة الحرة القياسية إلى أن المواد السطحية الكاتيونية الثلاثة المحضرة تمتص عن طريق الامتزاز الفيزيائي الكيميائي وان عملية الامتزاز تتبع منحنى الامتزاز ل (Langmuir). وعن طريق استخدام ميكروسكوب القوة الذرية (AFM) تبين انخفاض خشونة السطح بسبب طبقة الحماية المتكونة على سطح سبيكة النحاس-الألومنيوم-الزنك.